

widths, FWHM, of the $\text{Si}_{2p}^{\text{Si}}$, Si_{2p}^x , and $\text{Si}_{2p}^{\text{SiO}_2}$ are 1.1, 1.3–1.4, and 1.7 eV, respectively.

Two conclusions were obtained from these results. The first, drawn from the peak position of the Si_{2p}^x line, is that the chemical shift of Si atoms in the transition region is about 1.6 eV. In our other experiments, the true chemical shift of SiO_2 was 3.0 ± 0.2 eV.¹⁸ (Though the experimental chemical shift of the SiO_2 obtained from Fig. 2 was 3.5 eV, this value seemed to include the charging effect by x radiation. The method to obtain the true chemical shift was shown in detail in Ref. 18.) Thus, the chemical shift of the Si atoms in the transition region was about one-half that of those in SiO_2 .

The second conclusion, drawn from the peak intensity ratio $I(\text{Si}_{2p}^x)/I(\text{Si}_{2p}^{\text{Si}})$, is that the thickness of the transition region at the Si- SiO_2 interface is 0.2–0.3 nm thick. That is, the value for $d_x/\lambda_{\text{Si}_{2p}^x}$ obtained using the data in Fig. 2 and Eq. (1) was 0.087. Though the actual value of $\lambda_{\text{Si}_{2p}^x}$ is not known, it was assumed to be between 2 and 4 nm ($\lambda_{\text{Si}_{2p}^{\text{Si}}}$ was 2.3 nm at 1151 eV in kinetic energy and $\lambda_{\text{Si}_{2p}^{\text{SiO}_2}}$ was 3.5 nm at 1146 eV in electron kinetic energy in our other experiments¹¹). Thus, the thickness of the transition region, d_x was estimated to be 0.2–0.3 nm.

This transition region is considered to be a first monolayer of Si substrate in contact with SiO_2 film, because the thickness of the transition region is about the same as the atomic diameter of Si, and our other experimental result¹¹ shows that no O atoms are contained in this transition region.

To summarize the conclusions, it was clarified that the chemical shift for Si atoms in the transition region was 1.6 eV, and this value was about one-half of that of SiO_2 , and that the thickness of the transition region was 0.2–0.3 nm by studying the angular dependence of Si_{2p} photoelectron spectra.

The authors would like to express their gratitude to Mr. Katsuhisa Usami for ESCA measurements, to Dr. Shigehiko

Yamamoto for letting us use the ESCA instrument and discussions, to Dr. Kikuji Sato and Mr. Yōichi Takehana for fruitful suggestions and discussions.

¹R.A. Clarke, R.L. Tapping, M.A. Hopper, and L. Young, *J. Electrochem. Soc.* **122**, 1347 (1975).

²R. Flitsch and S.I. Raider, *J. Vac. Sci. Technol.* **12** 305 (1975).

³S.I. Raider and R. Flitsch, *J. Vac. Sci. Technol.* **13**, 58 (1976).

⁴F.J. Grunthaler and J. Maserjian, *IEEE Trans. Nucl. Sci.* **NS-24**, 2108 (1977).

⁵S.I. Raider and R. Flitsch, *IBM J. Develop* **22**, 294 (1978).

⁶J.S. Johannessen and W.E. Spicer, *J. Vac. Sci. Technol.* **13** 849 (1976).

⁷J.S. Johannessen and W.E. Spicer, *J. Appl. Phys.* **47**, 3028 (1976).

⁸C.R. Helms, Y.E. Strausser, and W.E. Spicer, *Appl. Phys. Lett.* **33**, 767 (1978).

⁹J. Blanc, C.J. Buicocchi, M.S. Abrahams, and W.E. Ham, *Appl. Phys. Lett.* **30**, 120 (1977).

¹⁰O.L. Krivanek, T.T. Sheng, and D.C. Tsui, *Appl. Phys. Lett.* **32**, 437 (1978).

¹¹A. Ishizaka, S. Iwata, and Y. Kamigaki, *Surf. Sci.* **84**, 355 (1979).

¹²L.C. Feldman, P.J. Silverman, J.S. Williams, T.E. Jackman, and I. Stensgaard, *Phys. Rev. Lett.* **41**, 1396 (1978).

¹³The “SiO” at the interface is different from “generally speaking” SiO. It is considered to be a first monolayer of Si substrate in contact with SiO_2 film, and it does not contain any O atoms.

¹⁴ $\langle \text{Si}_{2p} \rangle$, $\langle \text{Si}_{2p}^{\text{Si}} \rangle$, $\langle \text{Si}_{2p}^{\text{SiO}_2} \rangle$, and $\langle \text{Si}_{2p}^x \rangle$ stand for total Si_{2p} , $\text{Si}_{2p}^{\text{Si}}$, $\text{Si}_{2p}^{\text{SiO}_2}$, and Si_{2p}^x peaks, respectively.

¹⁵K. Siegbahn, U. Gelius, H. Siegbahn, and E. Olson, *Phys. Lett. A* **32**, 221 (1970).

¹⁶C.S. Fadley and S.A.L. Bergstrom, *Phys. Lett. A* **35**, 375 (1971).

¹⁷S. Iwata and A. Ishizaka, *J. Jpn. Inst. Metal.* **42**, 1020 (1978).

¹⁸S. Iwata and A. Ishizaka, *J. Jpn. Inst. Metal.* **43**, 380 (1979).

¹⁹S. Iwata and A. Ishizaka, *J. Jpn. Inst. Metal.* **43**, 388 (1979).

²⁰In previously reported works (see Ref. 11, 17, and 19), the true chemical shift of Si atoms in SiO_2 obtained was 3.0 ± 0.2 eV. Though the chemical shift of Si atoms in SiO_2 film obtained experimentally varied continuously from 3.5 to 4.7 eV with the increase of oxide film thickness from 1 to 3 nm, this change in the experimental chemical shift was interpreted in terms of electric charging by x radiation rather than as chemical state change. Furthermore, the oxide film on Si was found to be stoichiometric SiO_2 with a very thin (0.3-nm) layer of “SiO” at the Si- SiO_2 interface.

Arc annealing of BF_2^+ implanted silicon by a short pulse flash lamp

Juh Tzeng Lue

Department of Physics, National Tsing Hua University, Hsinchu, Taiwan, Republic of China

(Received 20 July 1979; accepted for publication 25 October 1979)

Step-junction diodes are obtained from BF_2^+ implanted silicon irradiated by a single pulse of light from a flash lamp. The FWHM is 100 μs with energy densities ranging from 12.4 to 20.6 J/cm². The sheet resistance and the I - V characteristic have been used to confirm the annealing process.

PACS numbers: 85.60. — q, 61.70.Tm, 81.40.Ef

Recently, laser annealing^{1–5} has been used as a powerful tool to correct flaws that are introduced during ion implantation. The Q -switched solid-state laser permits a localized short-pulse annealing on the thin layer near the surface. Thus, the drawbacks arising from conventional thermal an-

nealing such as inward diffusion of surface impurities and lateral diffusion of the implanted dopants can be eliminated. Laser annealing still has disadvantages of low pumping efficiency (usually less than 1% for a solid-state laser), expense, and small beam profile ($\sim 100 \mu\text{m}$ in diameter). For large-

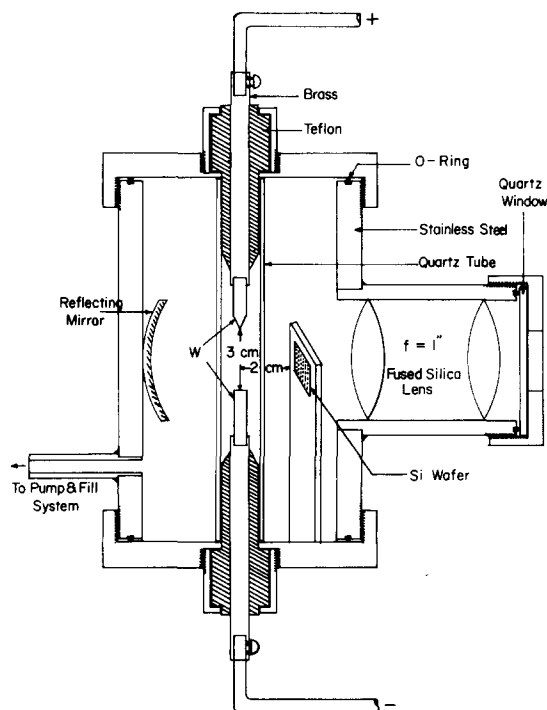


FIG. 1. Construction of a demountable flash lamp.

area processing and considering the economics, a high-energy-density short-pulse flash-lamp annealing might be more advantageous than laser annealing. So far as we know, there are only two papers concerning annealing by incoherent light sources.^{6,7} In the aforementioned work, preheating the sample at temperatures between 500 and 600 °C is required to allow complete regrowth. With the construction described here, a readily demountable flash tube provides a capacity for high-intensity irradiation and suffices for rapid annealing in one flash.

To induce a liquid-solid phase epitaxial growth from a thin amorphous Si layer, a threshold value of about 20 J/cm² should be reached for a pulse light of 50-μs duration. Longer pulse duration requires even higher light-energy density. In this study, a demountable flash lamp is designed as shown in Fig. 1. A gold-plated reflecting mirror is placed in back of the electrodes. A previous, aluminum coated mirror showed

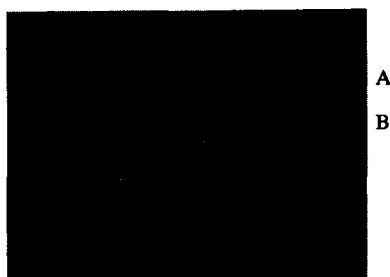


FIG. 2. Oscillograms of the current (A) and light pulse (B). Bank voltage: 1.4 kV, bank capacitance: 600 μF, vertical scale: 1.5 kA/div., horizontal: 50 μs/div., corresponding to an energy density of 12.4 J/cm² on the sample.

TABLE I. Sheet resistance of the arc annealed *n*-type silicon wafers implanted by BF₂⁺ ions with a dose of 1 × 10¹⁵/cm² at an energy density of 12.5 J/cm².

In energy (keV)	50	80	100	150
Sheet resistance (kΩ/□)	0.18	0.405	1.28	1.53

sputtering damage and evaporation after one or two flashes. The main electrodes are tungsten rods contained in brass rods which are press fitted into Teflon insulators for a vacuum seal. The Teflon loosely fits into a quartz tube, for the partial protection from shock waves. To obtain higher peak currents with even shorter pulse width for future studies, a spark gap or a thyatron could be connected in series with the flash tube to avoid self-breakdown when applying high voltage. The fill pressure of the argon gas should be kept below 50 Torr in order that the shock wave not destroy the wafers. In early work with samples placed at the focus point of the output-coupling lenses of the flash tube, wafers were not annealed successfully.

For a high-current short-pulse discharge system, the resistivity of the flash arc is given by Marotta's formula $V = kI^{0.85}$, where k is a constant of the tube.⁸ The normalized nonlinear differential equation for the circuit is⁹

$$\frac{dI}{d\tau} \pm \alpha' |I|^{0.85} + \int_0^{\tau} I d\tau = 1, \quad (1)$$

where

$$I = i(L_0/V_0), \quad Z_0 = (L_0/C_0)^{1/2}, \\ \tau = t/(L_0 C_0)^{1/2}, \quad \alpha' = (k/V_0^{0.15})(C_0/L_0)^{0.425},$$

L_0 is the circuit inductance, C_0 is the bank capacitance, and t is the time. The parameter α' determines whether the oscillation condition of the circuit will be underdamped, critical damped, or overdamped. It is found that to obtain maximum efficiency of the flash tube, the circuit should be critically damped. From our numerical calculations, $\alpha' \approx 1.3$ corresponds to the critical damped condition. Oscillograms showing the current and the light pulse measured by a Rogowski coil and a *p-i-n* photodiode, respectively, are shown in Fig. 2. The current is seen to be slightly underdamped and the oscillation will be greater if we increase either the operating voltage or the circuit inductance. The FWHM (full width at half-maximum) is about 100 μs.

The silicon samples ([111], 1–10 Ω cm, *n*-type) are implanted with BF₂⁺ ions. The energy of implantation ranged from a few tens of keV up to 180 keV with fluences ranging from 10¹⁴ to 10¹⁶ ions/cm². The incident angle of the ion beam is at about 7° so as to minimize channeling behavior. After exposure to the flash lamp, the wafers were cleaned in HF to remove the oxide layer and possible surface damage, and rinsed in acetone and then in deionized water. The sheet resistance of the sample surface clearly informs us of the impurity activation and lattice recrystallization, therefore the annealing results were examined by the four-point-probe method. Table I shows the partial recovery of the crystallization for different implanted ion energies at the same annealing energy density of 12.4 J/cm² (which is estimated by con-

TABLE II. Comparative data of the arc and isothermal annealings.

Arc annealing (150-keV BF_2^+ implanted at dose $1 \times 10^{14}/\text{cm}^2$).							
Energy density (J/cm^2)	7.68	10.7	12.4	14.2	16.2	18.3	20.6
Sheet resistance ($\text{k}\Omega/\square$)	283	13.3	1.38	1.1	0.99	0.58	0.46
Open-circuit voltage (V)	0	0.31	0.37	0.45	0.47	0.45	0.23
Isothermal annealing (120-keV BF_2^+ implanted at dose $1 \times 10^{15}/\text{cm}^2$, 750 °C annealed).							
Time (min)	1	2	7	12	17		
ρ_s ($\text{k}\Omega/\square$)	0.506	0.489	0.298	0.230	0.209		
V_{oc} (V)	0.32	0.44	0.46	0.48	0.49		

sidering the flash tube to be an ideal black-body radiator with 60% conversion efficiency of electrical energy to light).

Since the projected range $R_p(E)$ of the ions in the substrate and the straggling of the range $\Delta R_p(E)$ as predicted by the LSS⁹ theory increase as the incident ion energy increases, the depth of the amorphous layer also increases. Our results show that at this flash power, some repair of lattice damage takes place, but it is not possible to activate all of the carriers. The higher the implanted ion energy, the lower the annealing effect.

Table II shows that the sheet resistance steadily decreases as the exposing energy density increases from 7.68 to 20.6 J/cm^2 , demonstrating the increase of recrystallization from the amorphous condition and the activation of the impurities. A complete melting of the amorphous layer has not been achieved because the wafers are broken into small pieces when the bank voltage of the discharge circuit exceeds 1.8 kV with a bank capacitance of 600 μF . The photovoltaic open-circuit voltage V_{oc} of the wafer illuminated by AMI light has an optimum value of 0.47 V. Increasing the flash power above the critical condition, surface asperities by the bombarding argon ions increase the surface recombination velocity and consequently reduce the V_{oc} . Annealing data

for boron¹¹ indicates that temperatures in excess of 900 °C are needed if activation is to be achieved in a reasonable time. It is also clear that higher doses (i.e., $10^{15}/\text{cm}^2$ as opposed to $10^{14}/\text{cm}^2$) require substantially longer times to achieve the same level of activation. The isothermal annealing of the wafers at 750 °C as shown in Table II is compatible with the results of annealing by the incoherent light source.

The I - V plot as shown in Fig. 3 indicates that annealing at 20.6 J/cm^2 forms an ideal diode. With lower annealing energy density, the cut-in voltage and the dynamic resistance of the diode both increase. The $1/C^2$ vs V plot is a straight line which indicates that the junction has an abrupt doping profile. The total forward current for a p^+-n junction diode is¹²

$$J_F = q \left(\frac{D_p}{\tau_p} \right)^{1/2} \frac{n_i^2}{N_D} \exp \left(\frac{qV}{KT} \right) + \frac{qV}{2} \sigma v_{th} N_i n_i \exp \left(\frac{qV}{nKT} \right). \quad (2)$$

The two terms on the right-hand side represent the diffusion and generation-recombination currents, respectively. For silicon, n_i is small, and for a partially annealed diode, the

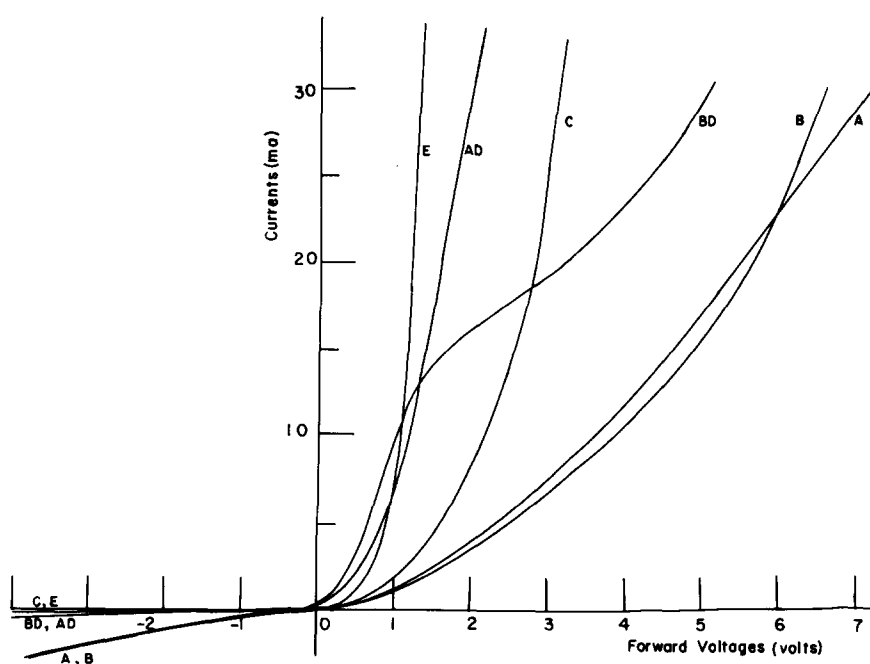


FIG. 3. The I - V characteristic of the arc annealed diode with flash-light energy density, A: 12.4 J/cm^2 , B: 14.3 J/cm^2 , C: 18.3 J/cm^2 , E: 20.6 J/cm^2 ; AD and BD correspond to A and B illuminated by AMI light, respectively.

minority diffusion constant D_p is small, and the concentration of the trapping centers N_t is large, so that the generation-recombination current will be the dominant term. Since n is greater than 1, the cut-in voltage and therefore the dynamic resistance will be higher for an incompletely annealed diode than for the ideal Shockley diode. This undesired large cut-in voltage has also been found in laser-assisted doping in silicon.¹³ When illuminated with AMI light, the forward characteristic shifts toward a lower dynamic resistance, showing that the photogenerated electron-hole pairs are captured by the trapping centers (N_t becomes small) and consequently, the forward current reduces to the diffusion current.

This work was supported by the Chinese National Science Council.

- ¹P. Baeri, S.U. Campisano, G. Foti, and E. Rimini, *J. Appl. Phys.* **50**, 788 (1979).
- ²J.C. Schultz and R.J. Collins, *Appl. Phys. Lett.* **34**, 84 (1979).
- ³R.T. Young, C.W. White, G.J. Clark, J. Narayan, W.H. Christie, M. Murakami, P.W. King, and S.D. Kramer, *Appl. Phys. Lett.* **32**, 139 (1978).
- ⁴J.R. Dennis and E.B. Hale, *J. Appl. Phys.* **49**, 1119 (1978).
- ⁵R.T. Young and J. Narayan, *Appl. Phys. Lett.* **33**, 14 (1978).
- ⁶H.A. Bombe, H.L. Berkowitz, M. Harmatz, S. Kronenberg, and K. Lux, *Appl. Phys. Lett.* **33**, 955 (1978).
- ⁷R.L. Cohen, J.S. Williams, L.C. Feldman, and K.W. Wost, *Appl. Phys. Lett.* **33**, 751 (1978).
- ⁸A. Marotta and K.M.O. Galvao, *Appl. Phys. Lett.* **33**, 15 (1978).
- ⁹D.Y. Song, J.T. Lue, and C.K. Yeh (unpublished).
- ¹⁰J. Lindhard, M. Scharff, and H.E. Schiott, *Phys. Rev.* **124**, 128 (1961).
- ¹¹T.E. Seidel and A.U. Mac Rae, *Radiat. Eff.* **7**, (1971).
- ¹²S.M. Sze, *Physics of Semiconductor Devices* (Wiley, New York, 1969), p. 104.
- ¹³K. Affolter, W. Lüthy, and M. von Allmen, *Appl. Phys. Lett.* **33**, 185 (1978).

Reduction of GaAs surface recombination velocity by chemical treatment

R.J. Nelson, J.S. Williams,^{a)} H.J. Leamy, B. Miller, H.C. Casey, Jr., B.A. Parkinson,^{b)} and A. Heller
Bell Laboratories, Murray Hill, New Jersey 07974

(Received 23 April 1979; accepted for publication 8 June 1979)

Chemisorbed ruthenium ions on the surface of n-GaAs decrease the surface recombination velocity of electrons and holes from 5×10^5 to 3.5×10^4 cm/sec. It is shown that the ions, in a one-third monolayer thickness, are confined to the surface and do not form a new junction by diffusing into the GaAs. This use of Ru appears to be the first observation of the reduction of the surface recombination velocity for GaAs by the simple chemisorption of ions.

PACS numbers: 73.20.Hb, 82.65.My, 68.45. — v

Surface recombination of carriers at the GaAs-air interface severely limits the performance of minority-carrier devices such as solar cells and detectors. This limitation may be overcome by growth of a layer of $\text{Ga}_{1-x}\text{Al}_x\text{As}$ on the air-exposed GaAs surface. The recombination velocity S at the GaAs- $\text{Ga}_{1-x}\text{Al}_x\text{As}$ interface is 450 ± 100 cm/sec,^{1,2} three orders of magnitude smaller than at the GaAs-air interface. Aside from this use of a lattice matched heterojunction, no other methods for the reduction of the surface recombination current are known. Common surface treatments, e.g., the growth of native oxides and the deposition of SiO_2 or silicon nitride, are known to alter the surface state density but have not been shown to decrease the surface recombination rate. For many applications however, overgrowth of a heteroepitaxial layer is not practical. For the particular case of solar cells, calculations show that reduction of the surface recombination velocity from 10^6 to 10^4 cm/sec produces a large efficiency increase while further reduction yields only a small improvement in efficiency.³ We report here a method for reduction of the recombination velocity at the GaAs-air interface to $3.5 \pm 0.5 \times 10^4$ cm/sec by a simple chemical treatment of the GaAs surface. Surface recombination velocities are determined by photoluminescence time-decay measurements.^{1,2} To the best of our knowledge, this is the first instance in which a persistent improvement has been reported for GaAs. The chemical treatment used here has

previously been reported to enhance energy conversion efficiency of n-GaAs/ S^- - Se_x^- - OH^- /C liquid junction solar cells⁴⁻⁶ significantly.

The samples used in this work were $\text{Ga}_{0.4}\text{Al}_{0.6}\text{As}$ -GaAs- $\text{Ga}_{0.4}\text{Al}_{0.6}\text{As}$ heterostructures grown on (100) GaAs substrates by a near-equilibrium LPE process.⁷ All three layers were doped with Te. Hall measurements on similar samples give $n = 2 \times 10^{17}$ cm⁻³ for the GaAs layer. The top $\text{Ga}_{1-x}\text{Al}_x\text{As}$ layer was removed by HF etching to produce a GaAs-air interface. Photoluminescence time decay measurements were then made through a window etched in the GaAs substrate as shown in the inset of Fig. 1. A $\text{Ga}_{1-x}\text{Al}_x\text{As}$ laser emitting at a wavelength of 7900 Å was used as a photoexcitation source.⁸ Light of this wavelength penetrates the $\text{Ga}_{1-x}\text{Al}_x\text{As}$ layer and is absorbed in the GaAs layer. The time decay of the GaAs luminescence is measured using a photon-counting system⁹ with a response time of 0.3 nsec.

The luminescence decay time τ of the fundamental decay mode is given by¹

$$(1/\tau) = (1/\tau_B) + D_p(4\eta_0^2/d^2), \quad (1)$$

where τ_B is the lifetime of the GaAs material, D_p is the minority-carrier diffusion coefficient, d is the GaAs layer thickness, and η_0 ($0 < \eta_0 < \pi/2$) is determined from the